Research Article | Vol. 24, No. 19 | 19 Sep 2016 | OPTICS EXPRESS 21329

Optics EXPRESS

All-optical depth coloring based on directional gating

SUNGJIN LIM, MUGEON KIM, AND JOONKU HAHN*

School of Electronics Engineering, Kyungpook National University, 80 Daehak-ro, Buk-Gu, Daegu, 41566, South Korea
**jhahn@knu.ac.kr*

Abstract: In non-contacting depth extraction there are several issues, such as the accuracy and the measurement speed. In the issue of the measurement speed, the computation cost for image processing is significant. We present an all-optical depth extraction method by coloring objects according to their depth. Our system is operated fully optically and both encoding and decoding processes are optically performed. Therefore, all-optical depth coloring has a distinct advantage to extract the depth information in real time without any computation cost. We invent a directional gating method to extract the points from the object which are positioned at the same distance. Based on this method, the objects look painted by different colors according to the distance when the objects are observed through our system. In this paper, we demonstrate the all-optical depth coloring system and verify the feasibility of our method.

OCIS codes: (200.4560) Optical data processing; (230.1150) All-optical devices; (070.1170) Analog optical signal processing.

References and links

1. W. Osten and N. Reingand, *Optical Imaging and Metrology Advanced Technologies* (Wiley-VCH Verlag & Co., 2012).
2. O. Wulf and B. Wagner, "Fast 3D scanning methods for laser measurement systems," in *International Conference on Control Systems and Computer Science* (2003).
3. P. J. Keller, A. D. Schmidt, A. Santella, K. Khairy, Z. Bao, J. Wittbrodt, and E. H. K. Stelzer, "Fast, high-contrast imaging of animal development with scanned light sheet-based structured-illumination microscopy," Nat. Methods **7**(8), 637–642 (2010).
4. P. Henry, M. Krainin, E. Herbst, X. Ren, and D. Fox, "RGB-D mapping: using depth cameras for dense 3D modeling of indoor environments," Int. J. Robot. Res. **31**(5), 647–663 (2012).
5. F. Nex and F. Remondino, "UAV for 3D mapping applications: a review," Appl. Geomat. **6**(1), 1–15 (2014).
6. B. Curless and M. Levoy, "A volumetric method for building complex models from range images," in *SIGGRAPH '96 Proceedings of the 23rd Annual Conference on Computer Graphics and Interactive Techniques* (ACM, 1996), pp. 303–312.
7. J.-H. Park, S. Jung, H. Choi, Y. Kim, and B. Lee, "Depth extraction by use of a rectangular lens array and one-dimensional elemental image modification," Appl. Opt. **43**(25), 4882–4895 (2004).
8. D. Shin and B. Javidi, "Three-dimensional imaging and visualization of partially occluded objects using axially distributed stereo image sensing," Opt. Lett. **37**(9), 1394–1396 (2012).
9. B. Wieneke, "Volume self-calibration for 3D particle image velocimetry," Exp. Fluids **45**(4), 549–556 (2008).
10. G. W. Scherer, "Structured-light 3D surface imaging: a tutorial," Adv. Opt. Photonics **3**(2), 128–160 (2011).
11. H. Choi, E. Y. Yew, B. Hallacoglu, S. Fantini, C. J. R. Sheppard, and P. T. C. So, "Improvement of axial resolution and contrast in temporally focused widefield two-photon microscopy with structured light illumination," Biomed. Opt. Express **4**(7), 995–1005 (2013).
12. A. K. C. Wong, P. Niu, and X. He, "Fast acquisition of dense depth date by a new structured light scheme," Comput. Vis. Image Underst. **98**(3), 398–422 (2005).
13. E.-H. Kim, J. Hahn, H. Kim, and B. Lee, "Profilometry without phase unwrapping using multi-frequency and four-step phase-shift sinusoidal fringe projection," Opt. Express **17**(10), 7818–7830 (2009).
14. K.-I. Joo, C.-S. Park, M.-K. Park, K.-W. Park, J. S. Park, Y. Seo, J. Hahn, and H. R. Kim, "Multi-spatial-frequency and phase-shifting profilometry using a liquid crystal phase modulator," Appl. Opt. **51**(14), 2624–2632 (2012).
15. C. I. Chang, *Hyperspectral Imaging: Techniques for Spectral Detection and Classification* (Springer Science & Business Media, 2003).
16. V. C. Coffey, "Hyperspectral imaging for safety and security," Opt. Photonics News **26**(10), 26–33 (2015).

#269893 http://dx.doi.org/10.1364/OE.24.021329
Journal © 2016 Received 7 Jul 2016; revised 16 Aug 2016; accepted 31 Aug 2016; published 6 Sep 2016

Optics EXPRESS

17. Y. Oiknine, I. August, and A. Stern, "Along-track scanning using a liquid crystal compressive hyperspectral imager," Opt. Express **24**(8), 8446–8457 (2016).
18. A. A. Wagadarikar, N. P. Pitsianis, X. Sun, and D. J. Brady, "Video rate spectral imaging using a coded aperture snapshot spectral imager," Opt. Express **17**(8), 6368–6388 (2009).
19. X. Lin, G. Wetzstein, Y. Liu, and Q. Dai, "Dual-coded compressive hyperspectral imaging," Opt. Lett. **39**(7), 2044–2047 (2014).
20. C. Palmer and E. Loewen, *Diffraction Grating Handbook*, 6th ed. (Newport Co., 2005).

1. Introduction

Three-dimensional (3D) metrology has received lots of interests from many people since this is essential for 3D modeling in many areas such as inspection, diagnosis, 3D scanning, and 3D microscopy [1–5]. Various methods are available for 3D measurement and among them, noncontact optical depth extraction methods have distinct advantages to acquire 3D shape of objects during short time and nondestructively.

In most optical depth extraction, triangulation geometry is applied [6]. At one vertex, a point of the object is positioned and at the other two vertices, optical instruments are placed respectively. As two optical instruments, one optical detector is necessary at one vertex and there are alternative choices, an additional detector or a pattern generator at the other vertex. In the case that two optical detectors are used, it is required to find correspondent points between two images with disparity [7–9]. Therefore, this method is difficult to be applied to the object with solid color or the objects with repeating pattern. On the other hand, the pattern generator specifies a point on the object precisely by illuminating previously designed patterns, that is, structured illumination and there is a potential to measure 3D object with high accuracy [10].

In structured illumination methods, the image of the pattern captured by the optical detector is distorted resulting from the distance between the pattern generator and the optical detector. The amount of this distortion can be converted into the depth information. Many algorithms have been proposed to improve the speed and the accuracy of measurement [11,12]. Instead of only one pattern, a set of plural patterns is used to increase the accuracy, or to prohibit the ambiguity. For example, the phase-shifting technique has several parameters for generating the patterns, such as spatial frequency and phase [13,14]. In most cases, the amount of the distortion is simply proportional to the depth of objects. Therefore, computation is considered to be essential to calculate the amount of the distortion from one image or a set of several images.

Up to my knowledge, the study to fully optically extract the depth has not been reported yet. In conventional methods, the illumination pattern with structure functions as an optical encoder and the computation algorithm functions as a decoder. Therefore, we invented an optical decoder with a directional gating optics which consists of an imaging lens and an aperture and accepts only rays with a specified direction. In this paper, a simple line pattern is constructed by using a projection lens and a slit for illumination and the aperture in the decoder is also a line slit. Both slits move together and one is synchronized to each other. At a fixed time, we define both directions of illumination and detection with the encoder and the decoder. So it specifies some object points in 3D space. Then while the slits are swishing, the object points on the same depth are obtained and the resultant image is a section of the object according to the depth.

In this paper, we use color spectrum for representation of the depth information. In hyperspectral imaging, the measurement becomes a hyperspectral cube which is a space with the coordinates, x, y, and λ [15]. Some hyperspectral cameras are operated by spectral scanning and others are operated by spatial scanning [16,17]. But it is worth to note that some snapshot hyperspectral cameras are composed of coded aperture and dispersion optics to capture the space (x, y, λ) [18,19]. The difference between hyperspectral imaging and depth extraction is that for depth measurement, 3D space with (x, y, z) is concerned instead of

Optics EXPRESS

(x, y, λ). We are inspired by the techniques in hyperspectral imaging and we realize an optical conversion from z-coordinate to λ-coordinate. For this conversion, a dispersion optical element such as a blazed grating is used. In this paper, we explain the principle of depth coloring based on directional gating and demonstrate experimental results to verify its feasibility.

2. Directional gating method

In general, depth extraction methods are based on triangulation geometry to compute the depth information. Figure 1 shows a conventional setup for the depth extraction based on structured illumination [10]. The light source projects a specific pattern on the object. If the object has irregularities on its surface, the pattern captured by the camera is distorted since the camera is placed apart from the light source. The distortion is directly related with the depth of the object due to the geometric relationship. So, the depth of the object is calculated from the amount of the distortion. Therefore, the system extracts the depth information from the triangulation geometry with three points which are two reference points of a light source and a camera and an interested point at the object. In this triangle, the distance from the camera to the object is defined by

$$l = g \sin\theta_L / \sin(\theta_L + \theta_C). \tag{1}$$

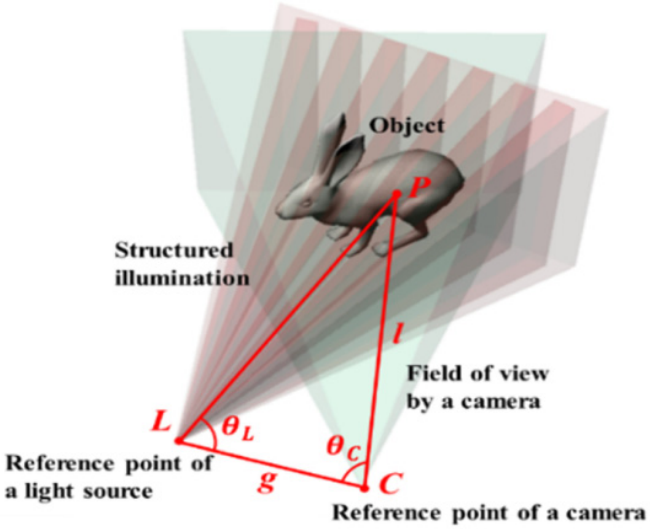

Fig. 1. Conventional setup for the depth extraction based on structured illumination.

Directional gating method is a novel way to selectively accept optical rays with a specific direction. This is realized by an imaging lens and a mechanical slit. The position of the slit determines which direction of optical ray is accepted. This structure is important to measure the depth of the object optically. If the only chief rays are concerned, every ray from the light source to the object is regarded to pass the center of the optical stop of the projection lens. Also the whole rays accepted by the camera are regarded to pass the center of the optical stop of the imaging lens. Therefore, the points at a fixed depth are chosen by directional gating.

Figure 2(a) shows a proposed structure of directional gating. The system consists of a projection part and a gating part. In each part, the slit is placed at the image plane of the lens. So the slit in the projection part makes a vertical line pattern on the object and its position depends on the place where the slit is opened. Then the direction of the pattern is changed by moving the slit from side to side. The slit in the gating part is a filter for selecting the only

Optics EXPRESS

specific depth information of the object by directional gating method. These two slits are physically linked and synchronized to each other. The projection lens and the imaging lens with correspondent slits function as optical encoder and decoder. The encoding process projects the specific pattern on the object. The decoding process accept the part of the projected pattern which is positioned at a specific depth. Here, two directional angles of the ray illuminating the object and the ray accepted by the camera identify the point with the same depth.

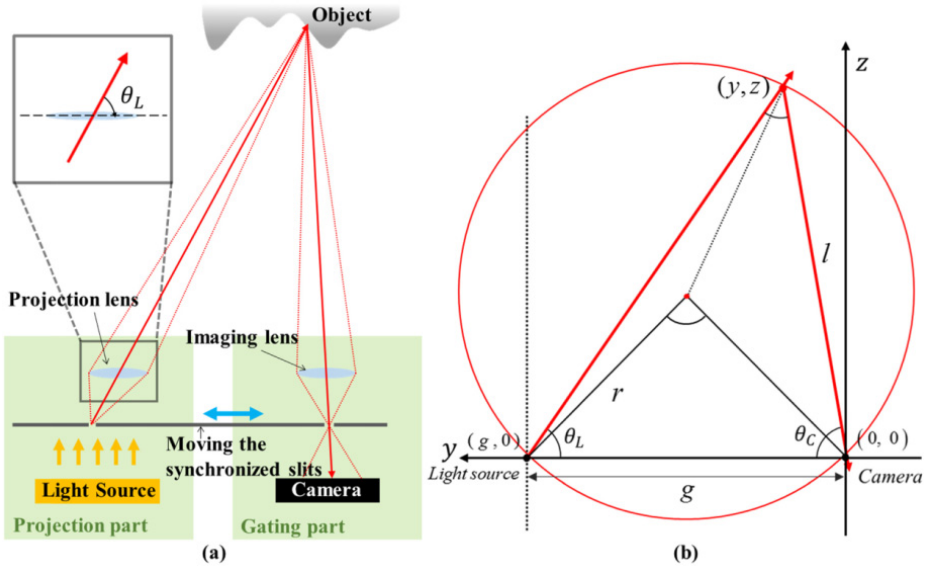

Fig. 2. (a) Structure of directional gating and (b) the circle of the positions selected by directional gating.

Figure 2(b) shows the circle of the positions selected by directional gating. The reference points of the projection part and the imaging part are located on $(g,0)$ and $(0,0)$ respectively. Here, g is the distance between these two reference points and θ_L is the angle between the direction of ray projected on the object and y-axis. θ_C is the angle between the reflected ray from the object to the camera and y-axis. There is a trade-off relation between the angle θ_L and the angle θ_C as follows

$$\theta_L + \theta_C = \theta_k. \tag{2}$$

The whole points satisfying Eq. (2) are placed on the circle. This is named depth circle where every points are captured by one swishing of the slits. This circle is defined as

$$\left(y - 0.5g\right)^2 + \left(z - 0.5\sqrt{4r^2 - g^2}\right)^2 = r^2. \tag{3}$$

Here, the radius r of the circle is given by

$$r = g/2\sin\theta_k. \tag{4}$$

Then, the distance from the reference point of the gating part to the object point and its depth along z-axis are respectively obtained as

$$l = 2r\sin\theta_L, \tag{5a}$$

Optics EXPRESS

$$z = (g - y)\tan\theta_L. \tag{5b}$$

From Eqs. (3) and (5b), the depth of the object point is simply represented as

$$z = \frac{l}{2r}\left[l\sqrt{1-(g/2r)^2} + g\sqrt{1-(l/2r)^2} \right]. \tag{6}$$

Since the illumination angle θ_L and the camera angle θ_C are physically constrained by the movement of the slits, the only object points on the depth circle are optically extracted during one swishig of the slit without any computation cost.

3. Depth coloring

Based on the directional gating method, we invent a way to get the depth information of objects wrapped by a rainbow color according to their depth. By adding a grating in the projection part, depth-coloring is realized as depicted in Fig. 3(a). The vertical line pattern which is defined by the slit and the lens turns into a rainbow spectrum after passing through the grating. The rainbow spectrum is projected on the object and then the part of reflected light with the specific direction is captured by the camera. The diffraction angle of the grating is related with the incident angle [20] and it is given as

$$\theta_m(\lambda) = \sin^{-1}(m\lambda/d + \sin\theta_i), \tag{7}$$

where d is a size of the grating blade and m is the order of diffraction. λ is the wavelength of incident light. θ_i and θ_m are an incident angle and diffraction angles according to the order of diffraction. In other words, the incident light is dispersed into a spectrum depending on the wavelength of the incident light. The longer the wavelength is, the larger the diffraction angle is. The illumination angle θ_L in the directional gating is an important parameter that effects on the extracted information. The illumination angle θ_L in the depth-coloring setup is obviously related with the diffraction angle and Eq. (2) becomes

$$\theta_m(\lambda) - \theta_C = \pi/2 - \theta_k. \tag{8}$$

The incident angle is determined by the position of the slit inside of the projection part and the directional gating angle θ_C is also determined by the position of the slit inside of the gating part. Since two slits are punctuated on a common plate, these two angles are related by

$$\phi_k = \pi/2 - \theta_i + \theta_C. \tag{9}$$

Here, ϕ_k is the bias angle and it is identified by the distance between two slits. The bias angle play an important role in adjusting the dynamic range of the depth.

Optics EXPRESS

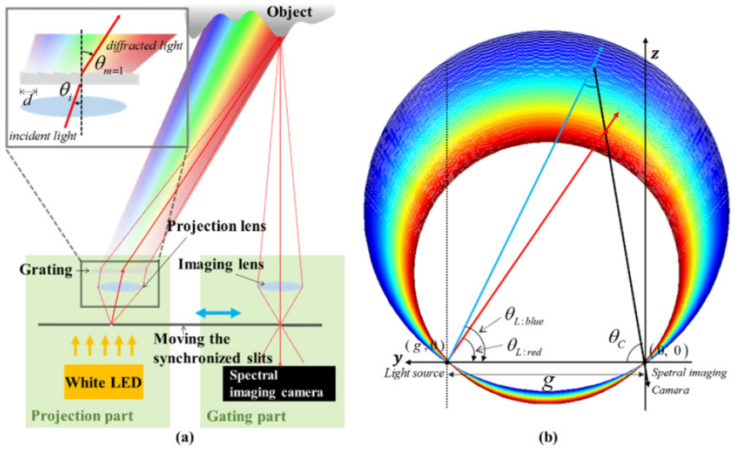

Fig. 3. (a) Structure of depth coloring and (b) the set of depth circles with different radii according to the selected wavelength.

In this paper, the only first order of diffraction is considered, that is to say $m=1$. From Eqs. (7)–(9), the radius of the circle in Eq. (4) becomes represented as

$$r=\frac{g}{2\sin\left[-\sin^{-1}\left(\lambda/d-\sin\theta_i\right)+\theta_i+\phi_k\right]}. \tag{10}$$

When the interested object is placed relatively far away from the camera such that r is much greater than g, the depth in Eq. (6) is approximately obtained by

$$z\approx\frac{g}{\sin\left(\lambda/d\right)\sin\phi_k}\sin^2\theta_L. \tag{11}$$

In Eq. (11), the relationship between z and λ brings about an intuition that the nearer the object is at the system, the longer wavelength is colored on the object. The size of the grating blade, d is closely related with the size of the dynamic range of the depth. According as the pitch of the grating decreases, the dynamic range of the depth increases. At the denominator, $\sin\phi_k$ represents the role of the bias angle. In this case, the bias angle is slightly smaller or larger than π and it is critical to adjust the center of the dynamic range of the depth. The existence of the last term, $\sin^2\theta_L$ means that the set of the object positions painted with the same color is curved depending on the angle of the light source. It brings about the error in conversion of the depth, z into the wavelength, λ. Figure 3(b) shows the geometry of depth circle according to the wavelength when the broadband light source is used. The radius of depth circle changes according to the wavelength. The depth circle for the red is smaller than that for the blue. Therefore, the depth information is converted into the color and the whole process is done without computation cost. Interestingly, it is possible for an observer to directly watch the object colored according to its depth through our system.

4. Experimental results

In order to verify the feasibility of the depth coloring method, we construct an all-optical system as shown in Fig. 4. The projection part and the gating part is configured in a box and the observer can watch the colored objects according to their depth through our system. As the light source, a cool white LED headlamp with 2,000 lumen manufactured by Moonlight is used. Two C-mount lenses with 25 mm fixed focal length manufactured by Computar are mounted on the box and they are used as the projection lens and the imaging lens. The gap

Optics EXPRESS

between two lenses, g is set 430 mm. The slit plate is placed on the roller and it moves manually. Two gratings with 300 l/mm and 600 l/mm from Edmundoptics are applied alternatively for the following experiments. As previously mentioned, the size of the grating blade, d determines the size of the dynamic range of the depth.

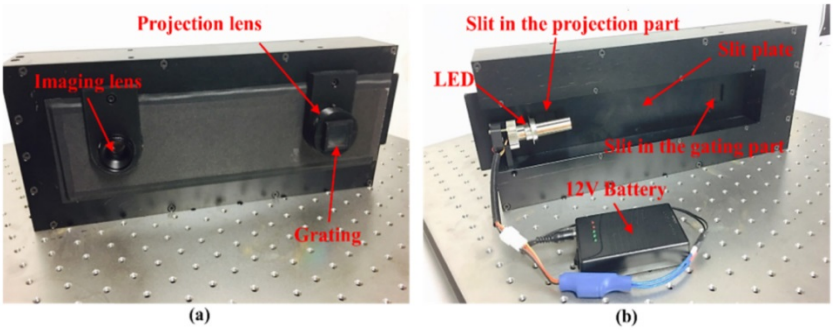

Fig. 4. All-optical depth coloring system with (a) a front view and (b) a back view.

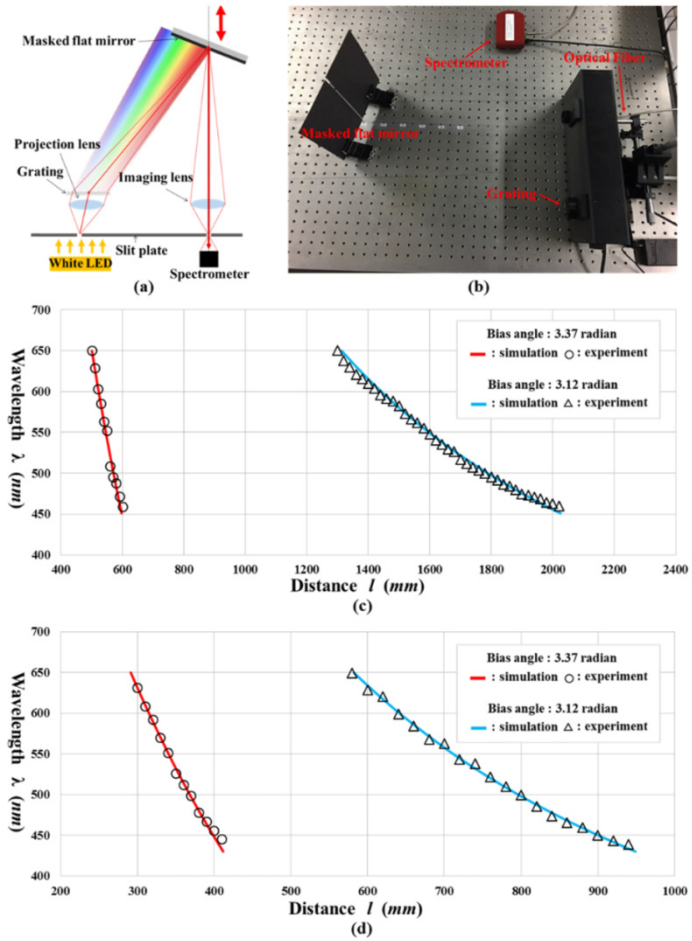

Fig. 5. (a) Schematic of the calibration experiment and (b) experimental setup. Relations between the distance of the mirror and the central wavelength of measured spectrum according to two bias angles when the gratings with (c) 300 l/mm and (d) 600 l/mm are applied.

Optics EXPRESS

To the calibration of the system, a masked flat mirror is used as an object and the wavelength of the reflected light is measured by a spectrometer as shown in Fig. 5(a). Except for the only narrow region of the mirror, the other region is blocked with the mask in order to exclude the noise resulting from the curvature of the depth circle. The reason why the mirror is used as an object is that enough light intensity is necessary for measuring the spectrum with a spectrometer. A compact CCD spectrometer manufactured by Thorlabs is used for this setup and the experimental setup for calibration is shown in Fig. 5(b). The relations between the distance of the mirror and the central wavelength of measured spectrum with two different gratings are shown in Figs. 5(c) and 5(d) respectively. In Fig. 5(c), the calibration data with two bias angles, 3.12 radians and 3.37 radians are presented when a grating with 300 l/mm is used. In the same manner, when a grating with 600 l/mm is used, the calibration data with two bias angles, 3.12 radians and 3.37 radians are shown in Fig. 5(d). The spectrum of the light source is measured in advance and the meaured spectrum is normalized. These graphs show that the central wavelength varies according to the depth in each condition. Here, the red line and the blue line represent the simulation results from Eq. (6) and the triangle and the square marks show the experimental measurements. The small difference between measurement and simulation is regardes as the result from the approximation of the lenses with cardinal points.

In this configuration, there are two parameters to determine the scope of the measurable depth. One is the bias angle and the other is the size of the grating blade. According as the bias angle decreases, the central value of the range of the depth increases. Since the central wavelength becomes insensitive to the depth according to the decrease of the bias angle, the dynamic ragne of the depth increases naturally. With a given central value of the range, the dynamic range decreases according as the size of the grating blade increases. Therefore, in order to aquire the depth-colored image, two parameters need to be carefully chosen depending on the objects.

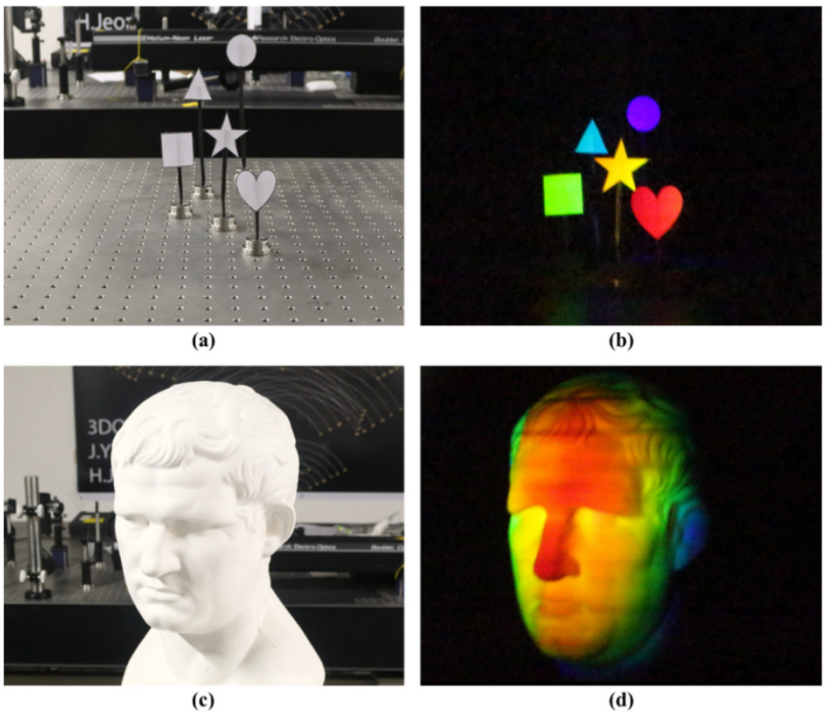

Fig. 6. (a), (c) Two objects for depth coloring experiment. (b), (d) Colored images through our system captured by a conventional camera.

Optics EXPRESS

Figure 6 exhibits the experimental results with all-optical depth coloring system. Two examples are examined and the depth-colored images are captured through the proposed system by a conventional camera. In the first experiment, five shapes of paper are used as the objects and these are placed at the different distance from the camera as shown in Fig. 6(a). For this experiment, the grating with 600 l/mm is applied and the bias angle is set 3.12 radians. A heart-shaped object is located at 600 mm, a pentagram-shaped object is located at 675 mm, a square-shaped object is located at 725 mm, a triangle-shaped object is located at 800 mm, and a circle-shaped object is located at 900 mm. Figure 6(b) shows the image measured by a camera. Here, the objects are colored in order as red, yellow, green, blue, and violet depending on their depth. The heart-shaped object located closest to the system is colored with red, the circle-shaped object located farthest to the system is tinged with violet. In the second experiment, another object with volume is examined which is a statue of Agrippa as shown in Fig. 6(c). Its range of the depth to be measured is small in comparison of that of the object in Fig. 6(a). To reduce the dynamic range of the depth, the grating with 300 l/mm is used. The distance between the system and the statue is about 500 mm. The bias angle is set 3.37 radians in consideration of the position of the statue. Figure 6(d) shows the experimental result and the rainbow spectrum appears on the statue. In detail, the nose and the forehead of the statue are colored with red. The right cheek is colored with green and yellow and the left cheek is colored with orange and green. The neck and the left ear are colored with blue. To compare the color spectrum of the objects with the calibration experimental results the same conditions are selected. From these experimental results, it is clear that the proposed method identifies the depth of the object by color.

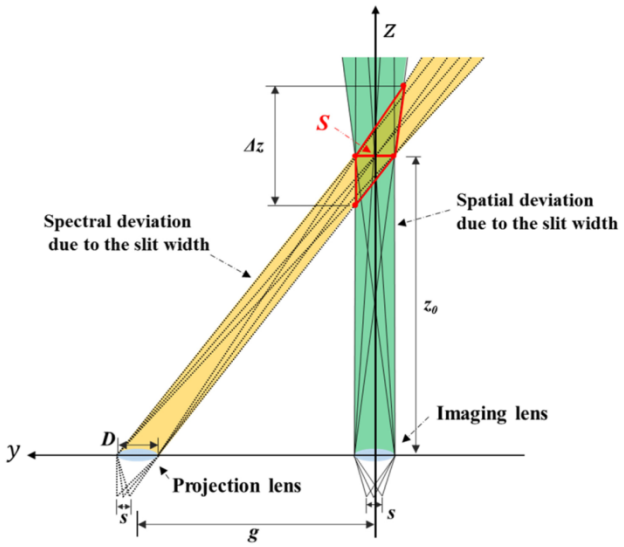

Fig. 7. Spectral and spatial deviations due to the width of the slits.

Figure 7 exhibits spectral and spatial deviations due to the width of the slits. Since the widths of the slits are determined to gather enough light intensity in consideration of the light source and sensor. On the object surface, the slit is projected by the projection part and then only specific rays passes through the slit in the gating part. Therefore, the accuracy of the depth coloring is defined by the spectral deviation in the projection part and the spatial deviation in the gating part. In addition, the aperture diameter, D of the lense brings about the error in depth coloring due to the confusion ring at defocused position. In Fig. 7, the overlap of these two deviation is geometrically identified by the width of the projection of the

Optics EXPRESS

slit, S at the focused depth position, z_0. So, the depth error is calculated from this overlap and it is given by

$$\Delta z = \frac{2(g-D)Sz_0}{(g-D)^2 - S^2} \approx \frac{2Sz_0}{g-D}. \tag{12}$$

The last approximation looks similar to the transverse resolution in optics since the focused depth, z_0 is possessed by the nominator and the aperture diameter, D and the gap between the lenses, g are placed in the denominator. But this is just the consequence of the analysis in ray optics. So, it is improper to compare it with the transverse resolution in wave optics.

When depth coloring method is applied to the object, there are some practical limitations. First, this method is significantly dependent on the reflectance of the light from the object. Therefore, ambient light disturbs the measurement and to overcome this noise, the modulation of the light source and lock-in detection may be an available solution to overcome. But this approach is beyond our original intention, all-optical process. Another limitation is the restriction of the objects. If the object has very low reflectance at a specific wavelength, some depth of an object correspondent to the wavelength cannot be extracted. For example, the object painted in red mainly reflects only red spectrum. So its depth is impossible to be measured by our method.

As previously mentioned, there is the conversion error from the depth to the color due to the curvature of the depth circle. It is a challengeable problem and it is expected to be improved by modifying the geometry of gating part in order to make the points with the same color become flat. Currently, two slits moves simultaneously and the same lenses are applied in the projection part and the gating part. So the angles θ_L and θ_C are tightly related by Eq. (2). If we apply electrical devices instead of mechanical slits, it is possible to control two slits independently. For example, digital micro-mirror device (DMD) generates a reflective narrow line and this line can play a similar function as the slit. So, if we control these angles as follows

$$\cot\theta_L + \cot\theta_C = g/z, \tag{13}$$

the conversion error can be eliminated.

In this paper, we move the slits manually and a round trip of them takes about 0.5 seconds and the exposure time of the camera is set 0.5 seconds. Therefore, the manual movement becomes a practical limit of the acquisition time. Because the exposure time of the focal plane array (FPA) sensor can be set much smaller than one second, there is a room to reduce the acquisition time by changing the mechanism of the slit. In future, we have a plan to upgrade our system with two digital micro-mirror devices (DMDs), each of which represents the dynamic movement of the slit. Since the DMD generates thousand binary patterns of the slit during one twentieth seconds, the limit of the acquisition time is expected to be around 50 milliseconds.

5. Conclusion

In this paper, we presented an all-optical depth coloring by a directional gating method. The directional gating method extracts the points from the object which are positioned at the same distance and the points look painted with the same color. Our system has a distinct advantage to extract the depth information in real time without any computation cost. It consists of a projection part and a gating part. The projection part illuminates the object with the rainbow spectrum and this spectrum pattern is swishing according to the movement of the slit in front of the surface light source. The gating part selects the specific part of spectrum by using an imaging lens and a slit which moves synchronized to the slit in the projection part. We demonstrated experimental results and confirmed the feasibility of our method. In our system,

Optics EXPRESS

two slits in projection part and gating part are physically linked to each other and the points in the cylinder are painted with the same color. In future, we will change the geometry of gating part and apply electrical devices such as DMD instead of mechanical movements. We expect the conversion error be solved by making the points with the same color become flat

Funding

Samsung Research Funding Center of Samsung Electronics (SRFC-IT1301-07).